

# Controlling a FCC/fluid-interface with umbrella sampling: A simulation study on the crystallization and melting of nearly hard spheres

Winston Oudshoorn

Daily Supervisor: Gabriele Coli & Professor Marjolein Dijkstra

## Abstract

Using simulations, we study the fluid/solid-interface in which the particles interact with the Weeks-Chandler-Andersen potential. We measure the average local bond order parameters were measured to study their behaviour at the interface between the two coexisting bulk phases. Subsequently, we employ the umbrella sampling technique using the globally averaged bond order parameters to investigate crystal growth and crystal melting of this system.

## Contents

<b>1</b>	<b>Introduction</b>	<b>2</b>
1.1	Research Questions . . . . .	2
<b>2</b>	<b>Theory</b>	<b>2</b>
2.1	Local Bond Order Parameters . . . . .	3
2.2	Averaged Local Bond Order Parameters . . . . .	4
2.3	Interface . . . . .	5
<b>3</b>	<b>Computational Methods</b>	<b>5</b>
3.1	Monte Carlo . . . . .	7
3.2	Metropolis . . . . .	7
3.3	Verlet List . . . . .	9
3.4	Umbrella Sampling . . . . .	9
	3.4.1 Global average bond order parameter . . . . .	10
	3.4.2 Umbrella sampling constant . . . . .	11
3.5	Parameters . . . . .	11
<b>4</b>	<b>Results and Discussion</b>	<b>13</b>
4.1	Case: $\frac{1}{2}\bar{q}_{l,FCC} + \frac{1}{2}\bar{q}_{l,fluid}$ ; $\kappa = 0.2$ . . . . .	13
4.2	Case: $\frac{3}{4}\bar{q}_{l,FCC} + \frac{1}{4}\bar{q}_{l,fluid}$ ; $\kappa = 0.2$ . . . . .	17
4.3	Case: $\frac{1}{4}\bar{q}_{l,FCC} + \frac{3}{4}\bar{q}_{l,fluid}$ ; $\kappa = 0.5$ . . . . .	20
4.4	Case: $\frac{1}{4}\bar{q}_{l,FCC} + \frac{3}{4}\bar{q}_{l,fluid}$ ; All umbrella sampling constants . . . . .	24
<b>5</b>	<b>Conclusion</b>	<b>28</b>

# 1 Introduction

In simulations of soft matter, the ability to distinguish different phases is necessary to analyze the system and for the use of a number of sampling techniques. Especially in simulations which focuses on multiple phases or on the interface between two phases, this ability is required to make proper conclusions about the system and the interface.

For this a theoretical approach is needed which accurately determines per particle whether it can be considered to be in a solid-like state or in a fluid-like state. This is achieved through a parametrization of the local symmetry of the environment surrounding the particle. This categorization can be done using local bond order parameters, or Steinhardt order parameters.<sup>6</sup> These bond order parameters are based on the local environment of the particle since its nearest neighbours determine whether it belongs to a fluid-like or a crystalline phase, and what type of crystalline phase in particular. Adjustments have been made to this method to improve its accuracy resulting in the averaged local bond order parameters which includes the local symmetry of the second nearest neighbours.<sup>4</sup>

These order parameters are able to accurately determine which phase a particle resides in if it is surrounded by a bulk phase, however at the interface of different phases the behaviour of these order parameters is not well known.

In this paper, an attempt will be made at simulating the behaviour of the interface between a bulk fluid-like phase and a bulk FCC-crystalline phase using a Monte Carlo simulation. This simulation will be analysed to observe the change of the averaged local bond order parameters at the interface. Furthermore a sampling technique called umbrella sampling will be applied to the system to examine crystal growth and crystal melting by shifting the location of the interface. This shift should not lead to a destabilisation of the system as at equilibrium the location of the interface is free to relocate. For a many-particle system to be simulated, computational limitations have to be taken into account as well to remain within the feasible time constraints.

## 1.1 Research Questions

These goals can be summarized in a number of research questions, thus:

1. How do the averaged local bond order parameters change for an interface between a fluid and an FCC phase?
2. Can umbrella sampling be used to shift the location of the interface and to study crystal growth and crystal melting?

## 2 Theory

In order to grasp what might happen at the interface between the two bulk phases, the usage of local bond order parameters is necessary. In particular the theory of averaged bond order parameters will be used for the analysis of the system.

The interface between the phases can be analysed by the transition the parameters go through as the environment surrounding particles changes from a bulk FCC-crystalline phase to a bulk fluid phase. As part of the theory of averaged local bond order parameters, a particle can be accurately classified as being in a fluid-like phase or in a solid-like phase through the use of an

order parameter, which does not have a high selectivity for specific crystalline phases, but instead has a high selectivity for either a solid-like phase or a fluid-like phase.<sup>1</sup>

The theory of averaged local bond order parameters parametrises the local symmetry of the environment of the particle in bulk phases accurately, enabling an analysis of the interface through the change these parameters go through from one bulk phase to the other.

## 2.1 Local Bond Order Parameters

The theory behind bond order parameters is well developed and computational studies of phase changes often incorporate these to effectively distinguish which phase a particle belongs to. Bond order parameters are a set of parameters based on spherical harmonics to describe the local and extended orientational symmetries displayed by crystalline structures. The bond order parameters utilize local symmetries for its description of the phase a particle resides in. This requires a frame of reference from the particle itself, and not from the frame of reference of the system. The calculations use the invariants of the spherical harmonics which negates the need for an external frame of reference, making the perspective of the particle itself the frame of reference for the calculation of these parameters.<sup>6</sup> For this approach the following algorithm was developed.

First a complex vector  $q_{lm}(i)$  of the  $i^{\text{th}}$  particle is defined as follows:

$$q_{lm}(i) = \frac{1}{N_b(i)} \sum_{j=1}^{N_b(i)} Y_{lm}(\mathbf{r}_{ij}) \quad (1)$$

Here  $N_b(i)$  is the number of neighbours of particle  $i$ ,  $\mathbf{r}_{ij}$  is the vector between particle  $i$  and its neighbour  $j$ , and  $Y_{lm}$  are the spherical harmonics. As for the parameters  $l$  and  $m$ ,  $l$  is an integer and  $m$  is an integer which goes from  $-l$  to  $l$ .

Note that  $l$  and  $m$  refer respectively to the degree and order of the spherical harmonics. This complex vector will be further developed into the bond order parameters below.

The local bond order parameters which contain the information of the local structure are defined as follows:

$$q_l(i) = \sqrt{\frac{4\pi}{2l+1} \sum_{m=-l}^l |q_{lm}(i)|^2} \quad (2)$$

where  $q_{lm}(i)$  is defined above, and  $q_l(i)$  is the bond order parameter of order  $l$  for the  $i^{\text{th}}$  particle. The integer  $l$  generally dictates for which crystal structure the parameter  $q_l$  can be sensitive. This is solely dependent on the angles between particles and thus requires no outside frame of reference. The cases of  $l = 4$  for  $q_4$  and  $l = 6$  for  $q_6$  are often used to distinguish between cubic and hexagonal structures. Note the invariant form of the complex vector being used to cause the particle in question to be the frame of reference for its environment and local symmetry calculation.

At the cost of selectivity for the specific crystal structure, a high selectivity can be achieved for either the solid-like phase or the fluid-like phase using the a scalar product,  $S_{ij}$ .<sup>1</sup> This is able to distinguish more accurately particles at the interface belonging to the solid phase or the fluid

phase, and can be used in addition to the order parameters themselves to observe the transition of the phases. It is defined as the scalar product,  $S_{ij}$ :

$$S_{ij} = \sum_{m=-6}^6 q_{6m}(i)q_{6m}^*(j) \quad (3)$$

where  $q_{6m}^*$  indicates the complex conjugate of  $q_{6m}$ . The scalar product  $S_{ij}$  is calculated for a particle  $i$  and one of its neighbours  $j$ , considering those particles to be connected if  $S_{ij} > 0.5$ . If a particle has more than a threshold number of connections it can be considered solid-like. This number is generally between 6 and 8,<sup>4</sup> but both the value of  $S_{ij}$  for connectedness and the threshold number are dependent on crystal structure and can differ significantly per solid. This might significantly increase the selectivity for distinguishing between solid-like phases and fluid-like phases.

The local bond order parameters have the drawback that thermal fluctuations widen their distribution considerably. This widening needs to be attenuated so that distributions of different crystal structures do not overlap considerably. To that end an averaging procedure was developed to accurately determine the crystal structure.<sup>4</sup> These are called the averaged bond order parameters and will be discussed below.

## 2.2 Averaged Local Bond Order Parameters

The averaged local bond order parameters closely follow the procedure of the local bond order parameters. It starts with an averaged complex vector which is defined as follows.

$$\bar{q}_{lm}(i) = \frac{1}{\tilde{N}_b(i)} \sum_{k=0}^{\tilde{N}_b(i)} q_{lm}(k) \quad (4)$$

Here,  $\tilde{N}_b(i)$  refers to the neighbours of particle  $i$  plus particle  $i$  itself, so that the average complex vector is calculated over the entire neighbourhood of particle  $i$ . The averaged local bond order parameter is defined as:

$$\bar{q}_l(i) = \sqrt{\frac{4\pi}{2l+1} \sum_{m=-l}^l |\bar{q}_{lm}(i)|^2} \quad (5)$$

Because the averaged local bond order parameter averages over the local bond order parameters of the nearest neighbours, it takes into account the local symmetry of the second-nearest neighbours of the particle. The information provided by including the second-nearest neighbour shell serves two purposes.

In the averaging process the information of the local bond order parameter of particle  $i$  is averaged with the added information of the local bond order parameter of the neighbours, which leads to a decreased accuracy of the local bond order parameters at the exact position of the particle. However the local bond order parameters at any exact position are under the influence of thermal fluctuations, and as such have diminished value in determining whether or not a particle might belong to a specific crystalline phase or a fluid phase.

Subsequently it is because of the averaging process and the bond order parameters being determined as an average of the neighbourhood surrounding a particle, that the effects of thermal fluctuations are minimised and the determination of which specific phase the particle belongs to becomes more accurate.<sup>4</sup>

## 2.3 Interface

There is no clear theory on what is expected to happen for the averaged local bond order parameters in the case of an interface layer between two bulk phases, however there are some suppositions that can be made. In the following table data is reported by Lechner *et al.*<sup>4</sup> for the averaged local bond order parameters for a Lennard Jones liquid and a number of crystal structures, all under the same pressure and temperature.

Table 1: Averaged bond order parameters of different phases of  $l = 4$  and  $l = 6$

	$\bar{q}_4$	$\bar{q}_6$
BCC	0.033406	0.408018
FCC	0.158180	0.491385
HCP	0.084052	0.421813
Liq.	0.031246	0.161962

What is shown are the means of the distributions for the averaged local bond order parameters of the body centred cubic (BCC), face centred cubic (FCC), hexagonal closest packed (HCP) crystal structures, and the undercooled liquid (Liq.) state. It displays the means for the cases of  $l = 4$  and  $l = 6$ .<sup>4</sup>

The interface between two bulk phases is expected to transition between the values of the means of their distributions. This transition is expected to be at least as wide as the interface itself as particles residing in the interface do not have a clearly defined bulk phase environment. Nevertheless as the interface layer is expected to be thin in comparison to the bulk phases, the transition is expected to be sharp. We perform a simulation of a fluid-like bulk phase and a FCC crystalline bulk phase which are separated by an interface. If the bulk fluid-like phase is comparable to the liquid phase, it will have a  $\bar{q}_6 \approx 0.161962$  and  $\bar{q}_4 \approx 0.031246$ , while the bulk crystalline phase is expected to have  $\bar{q}_6 = 0.491385$  and  $\bar{q}_4 = 0.158180$ . The interface between the two bulk phases is then expected to have a sharp change between these two values, but quickly adopting these mean values again as soon as the environment of the particles reaches a bulk phase.

In order to simulate a stable interface, the bulk phases need to be properly simulated. In the next section, we discuss the methods for establishing a stable interface in simulations.

## 3 Computational Methods

The build up of the simulation is of primary importance to ensure that the data gathered is not skewed or misrepresentative of the equilibrium situation, else any possible conclusion has no basis. In this section, we present the simulation methods to equilibrate a stable fluid-solid interface, while trying to use the computation time efficiently.

The system will be made through the simulation of a bulk fluid phase and a bulk FCC phase and subsequently combining these two in a single two-phase system. This as opposed to starting from a single phase and nucleating a secondary phase to create an interface. The reason for this is the timescale needed for the nucleation of a crystalline phase. For molecular dynamics simulations to observe a single nucleation could potentially require  $10^{24}$  time-steps for a moderately supersaturated system.<sup>1</sup> To avoid this time-consuming process and allow focus on the interface, a two-phase system will be created instead of nucleated.

The interaction potential between the particles is a modified Lennard Jones interaction called the Weeks-Chandler-Andersen interaction potential, or WCA potential, whose use is preferred over the Lennard Jones potential in this case for a number of reasons. It neglects interactions from a specific distance onwards, substantially decreasing computing time, at the cost of contributions to the energy interactions at long range. These contributions are not minor but they do approach zero at long range. This has as result that there is no gas-liquid transition, and here the gas or liquid can also be called a fluid phase. The Lennard Jones potential,  $\Phi_{LJ}$  has the form:

$$\Phi_{LJ}(r) = 4\epsilon\left[\left(\frac{\sigma}{r}\right)^{12} - \left(\frac{\sigma}{r}\right)^6\right] \quad (6)$$

where  $\epsilon$  is the depth of the potential well,  $r$  is the distance between the two particles,  $\sigma$  is a measure of the diameter of the particles and is equal to the Van der Waals diameter.

In the Weeks-Chandler-Andersen interaction potential,  $\Phi_{WCA}$ , the Lennard-Jones potential is cut off as follows:

$$\Phi_{WCA}(r) = \begin{cases} 4\epsilon\left[\left(\frac{\sigma}{r}\right)^{12} - \left(\frac{\sigma}{r}\right)^6\right] + \epsilon & \text{if } r < 2^{\frac{1}{6}}\sigma \\ 0 & \text{if } r \geq 2^{\frac{1}{6}}\sigma \end{cases} \quad (7)$$

where the variables and parameters are all equal to equation 6. This means that every interaction past the minimum of the potential well is ignored so that long range attractive forces are neglected.

The model of the simulation is that of a Markov process, a system whose variables, which in our case would be the coordinates of the particles, randomly change over time. This random process model will be used in conjunction with a Monte Carlo algorithm, giving rise to a Markov Chain Monte Carlo algorithm, which in our case is the Metropolis algorithm.<sup>3</sup> This section will include a description of Monte Carlo simulations and subsequently the Metropolis algorithm, as well as their necessity.

It would be a naive attempt to simulate a many-particles system and straightforwardly numerically integrate the ensemble averages. An ensemble average of an observable  $A$  is defined as:

$$\langle A \rangle = \frac{\int d\mathbf{r}^N A(\mathbf{r}^N) \exp[-\beta U(\mathbf{r}^N)]}{\int d\mathbf{r}^N \exp[-\beta U(\mathbf{r}^N)]} \quad (8)$$

where  $d\mathbf{r}^N$  would be the volume element of phase space,  $\exp[-\beta U(\mathbf{r}^N)]$  is the Boltzmann weight,  $\beta$  the inverse temperature,  $\frac{1}{k_B T}$ , where  $k_B$  is the Boltzmann constant and  $T$  temperature, and  $U(\mathbf{r}^N)$  is be the potential energy due to the interactions between the particles.

The problem would be that this integration should be performed over the entirety of phase space which is impossible to sample for any computer within any reasonable amount of time.<sup>2</sup> The

phase space grid must be sufficiently fine for an accurate sampling but at the same time the vast majority of phase space points has a very low Boltzmann weight as these phase space points contain particles coming close in range of each other, increasing the potential energy between particles due to the  $\frac{1}{r^{12}}$ -factor of the Weeks-Chandler-Andersen potential. It becomes necessary to implement specific numerical techniques, such as the Monte Carlo method.

### 3.1 Monte Carlo

In a Monte Carlo simulation the ensemble averages are calculated by integrating over a number of random phase space points instead of over all space. By letting the number of random phase space points grow very large an ensemble average can be calculated as follows,

$$\langle A \rangle = \lim_{n \rightarrow \infty} \frac{\sum_{i=1}^n A(\mathbf{r}_i^N) \exp[-\beta U(\mathbf{r}_i^N)]}{\sum_{i=1}^n \exp[-\beta U(\mathbf{r}_i^N)]} \quad (9)$$

where the parameters and variables are all the same as above, and  $n$  is the number of random samples. This is an unfeasible method in cases of dense fluids or solids as the majority of random samples would have a very low Boltzmann weight due to their close range.<sup>5</sup> However the step from integrating over all phase space to integrating over a number of random points has already severely improved the computability for a many-particle system. To make the computation feasible, the Metropolis-Hastings algorithm was devised, which will be discussed in the next section.

### 3.2 Metropolis

In the Metropolis algorithm, which is a modified Monte Carlo algorithm, the method no longer chooses configurations  $\mathbf{r}_i^N$  at random and then weighs them according to their Boltzmann factor,  $\exp[-\beta U(\mathbf{r}_i^N)]$ , as in an ordinary Monte Carlo simulation, but instead generates configurations with a probability  $\exp[-\beta U(\mathbf{r}_i^N)]$  and weighs them evenly.<sup>5</sup> This means that configurations  $\mathbf{r}_i^N$  are generated proportional to their probability<sup>2</sup>  $\exp[-\beta U(\mathbf{r}_i^N)]$  allowing the ensemble average calculation to be reduced to

$$\langle A \rangle = \lim_{n \rightarrow \infty} \frac{1}{n} \sum_{i=1}^n A(\mathbf{r}_i^N) \quad (10)$$

where the variables and parameters are the same as above, with the exception of  $n$ , which is now the number of samples, as the samples are no longer randomly generated. The generation of configurations is done as follows: At first an initial configuration is created in which a number  $N$  of particles are placed in a volume such that there is no close range overlap between particles causing large interaction energies due to the Weeks-Chandler-Andersen potential. Particles are then moved according to,

$$X_{i+1} \rightarrow X_i + (2\alpha_x - 1)\Delta \quad (11)$$

where  $X_{i+1}$  is any coordinate vector of the  $(i+1)^{th}$  configuration,  $X_i$  is the coordinate vector of the  $i^{th}$  configuration,  $\alpha_x$  is a random number between  $[0, 1]$ , and  $\Delta$  is the maximum allowed

displacement. Subsequently the potential energy change of the system caused by the move is calculated which we name  $\Delta E$ . This means to say that the interparticle energies between all particles according to the Weeks-Chandler-Andersen interaction potential is calculated for the  $(i+1)^{th}$  configuration and the energy for the  $i^{th}$  configuration is subtracted from that. If  $\Delta E < 0$ , the move causes the system to move to a lower energy state, and the move is accepted and the particle is moved. If however  $\Delta E > 0$ , the system would be brought to a higher energy state, and the move is allowed with the following probability:

$$acc(o \rightarrow n) = \min(1, \exp[-\beta(\Delta E)]) \quad (12)$$

where  $\beta$  is the inverse temperature, and  $\Delta E$  the change in energy. This probability is compared to a random number chose between  $[0, 1]$  and accepted if the probability is larger than the randomly chosen number, and rejected when the probability is smaller than the random number.

This probability is the ratio of the new and old Boltzmann weight. To do this a random number,  $\xi$ , is chosen in the range  $[0, 1]$  and compared to the Boltzmann weight. If  $\xi < \exp[-\beta(\Delta E)]$  the move is accepted and the particle is moved, and if  $\xi > \exp[-\beta(\Delta E)]$  the move is rejected and the particle is not moved at all.<sup>5</sup> This method of sampling greatly increases the efficiency of the Monte Carlo simulation while retaining the necessary physics such as ergodicity.

Having developed a physically valid and computable method for the change in configurations, a description can be made for the build up of the program. This change from one configuration to another is referred to as a move. In the simulation two kinds of moves exist: A "move", which is the attempt of moving one particle from its current coordinates to a new set of coordinates, and a "volume move", which consists of attempting to change the current volume into a different volume, which changes all interparticle distances. The description of a move has been given above already, the description of a volume move is given below.

In the case of a volume move, the volume is changed by a random amount as prescribed below:

$$V_{i+1} = V_i + (2\alpha - 1)\Delta v \quad (13)$$

where  $V_{i+1}$  is the volume of the  $(i+1)^{th}$  configuration,  $V_i$  is the volume of the  $(i)^{th}$  configuration,  $\alpha$  is a random number between  $[0 - 1]$ , and  $\Delta v$  is the maximum allowed volume change. The ratio  $(V_{i+1}/V_i)^{\frac{1}{3}}$  is used as the factor by which all the sides of the volume are changed, after which the same is done to all the coordinate vectors of the particles. This will change the interparticle distances, thus changing the energy of the system. The acceptance rule for the volume differs from that of the ordinary moves however due to the volume change,  $\Delta V = V_{i+1} - V_i$ . Whereas in the ordinary move comparison the case  $\Delta E < 0$  would result in readily accepting the move, for volume moves the change in volume has to be taken into account. This results in moves being accepted with the probability:

$$acc(V \rightarrow V') = \min(1, \exp[-\beta(\Delta E + P(\Delta V) - N\beta^{-1} \ln(V_{i+1}/V_i))]), \quad (14)$$

where  $P$  is the pressure of the system which is fixed. This probability is, like the move comparison, compared to a random number chosen between  $[0, 1]$ , and when this probability is larger, the volume move is accepted. If the move is rejected, all the particles are placed back at their initial positions and the volume is changed back to its original value.<sup>2</sup>



At this point the physical sampling of the simulation is complete and proper simulations can be run using this set up. Some computational advantage can be achieved through the use of Verlet lists over traditional neighbour searching methods. For the system in this case as well, the Boltzmann-weighted sampling can be improved through means of non-physical sampling. This is called umbrella sampling and will be discussed in a following section.

### 3.3 Verlet List

In order to compute the bond order parameters, it is necessary to find each neighbour of a particle as to determine what constitutes its local environment. There are many methods for finding neighbours in many-particle systems, the most straightforward being to consider all particles within a given cut off radius to be a neighbour of the particle<sup>1,4</sup>. This method has its disadvantages, for our case the computational time required to loop through the entire system for each particle makes it unfeasible within the time constraint. Yet it is required to accurately find each neighbour of a particle in order to determine its local environment. Without a proper determination of the local environment it becomes impossible to have accurate results for the bond order parameters. To decrease the computation time the use of Verlet lists is used.

For each particle a Verlet list is created, consisting of each particle within a large cut off radius. In our case specifically for a particle  $i$ , a particle  $j$  is considered to be part of the Verlet list if the distance  $dr_{ij} = |\mathbf{r}_i - \mathbf{r}_j|$  between the two particles is smaller than the following cut off radius:

$$\frac{dr_{ij}}{\sigma} \leq 2^{\frac{1}{6}} + 0.9 (\approx 2.0225) \quad (15)$$

so that within this large cut off radius every particle is counted into the Verlet list. Subsequently from those Verlet lists the neighbours are determined using the following equation:

$$\frac{dr_{ij}}{\sigma} < 1.4. \quad (16)$$

If this were done for each move, the use of Verlet lists would actually increase computation time. However due to the larger cut off radius, as long as the particle has not moved too far from its original position, the Verlet list can be used for a multiple of moves so that the neighbour searching per move is done over the smaller number of members of the Verlet list and the more computationally intensive process of looping over the entire set of particles to construct the Verlet list is done less often. Specifically if a particle has strayed a total distance in any direction larger than  $0.45\sigma$  from its original position, the Verlet necessarily needs to be reconstructed to ensure all members of the Verlet list are included. This set up of using two lists of consisting of a larger Verlet list reconstructed after a number of moves by looping over all particles and the subsequent result of a small list of actual neighbours constructed every move by looping over all the members of the Verlet list substantially decreases computation time without decreasing accuracy. For this reason the method of Verlet lists is included for our case.

### 3.4 Umbrella Sampling

Umbrella sampling is a non-physical means of sampling. This means that the weighting assigned to configurations deviates significantly from the probability these configurations would have had

in reality. This has the advantage of decreasing computation time by a large margin for the same Monte-Carlo experiments done solely by assigning the appropriate Boltzmann weights to configurations, and the disadvantage that certain configurations will be more probable than they would have been in reality.<sup>7</sup> We will use umbrella sampling together with the bond order parameters as a parameter to attempt to shift the location of the interface, as well as to study crystal growth and crystal melting.

The umbrella sampling potential is added to the energy of the previous configuration, and recalculated at the next configuration, so that when the energies are compared, moves which would lead to increasing the potential would more often be rejected than moves which would decrease the potential. The form of the potential well is as follows:

$$\beta V_{pot}(\bar{q}_l) = \frac{1}{N} \sum_{i=1}^N \kappa (\bar{q}_l(i) - \bar{q}_{l,target})^2 \quad (17)$$

where  $\kappa$  is a dimensionless constant chosen such that the umbrella sampling could have a large impact on the total energy of the system,  $\bar{q}_{l,target}$  is the target value for the specific  $\bar{q}_l$  for a particle  $i$  which is the averaged bond order parameter as defined in equation 5. The potential  $V_{pot}$  is added to the energy of the system. Umbrella sampling potentials are only calculated over  $l = 4$  and  $l = 6$  and not using any other value of  $l$ . Using only the local values of the averaged bond order parameters has a possible disadvantage. If the umbrella sampling potential is too large, it might induce local (dis)ordering in the bulk phases as every move moving the averaged bond order parameters towards the target bond order parameters is accepted. To avoid this, an averaging procedure is used so that the probability of moves in the bulk phase being accepted are attenuated by the rest of the system. This leads to a global average bond order parameter, and is discussed below.

### 3.4.1 Global average bond order parameter

Using umbrella sampling for each averaged local bond order parameter has the result that each and every particle, whether it resides in the interface, near the interface, or within the bulk is given the same added potential if they happen to have the same local bond order parameter. This inevitably creates the same driving force on particles residing in the bulk as it does on particles residing near the interface, so that if the umbrella sampling potential is too strong, for example due to a high  $\kappa$ , an entire bulk phase can be caused to phase change, for example causing the FCC-phase to melt entirely. To ensure this effect does not occur it becomes necessary to attenuate the umbrella sampling over the entire system so that moves causing a large difference in bond order parameters, such as moves in the neighbourhood of the interface, are generally more accepted than moves within the bulk which generally do not cause large differences in bond order parameters. This decreases the possibility of bulk phase changes caused by umbrella sampling although it does not entirely negate it if the umbrella sampling constant  $\kappa$  is set too high. This attenuation is done by not constructing the potential well around  $\bar{q}$  of each particle separately as done in equation 17 but instead by averaging over all bond order parameters and subsequently using this globally averaged bond order parameter in the umbrella sampling potential:

$$\bar{q}_l^{global} = \sum_{i=1}^{i=N} \frac{\bar{q}_l(i)}{N} \quad (18)$$

where  $\bar{q}_i^{global}$  is the globally averaged averaged local bond order parameter,  $\bar{q}_l(i)$  is the averaged local bond order parameter of the  $n^{th}$  particle, and  $N$  is the number of particles of the system. Subsequently  $\bar{q}_i^{global}$  is used in the calculation of the umbrella sampling potential:

$$\beta V_{pot}(\bar{q}_i^{global}) = \kappa(\bar{q}_i^{global} - \bar{q}_{l,target})^2 \quad (19)$$

where the parameters are the same as equation 17. This attenuation decreases the probability for bulk phase changes and makes it more likely for phase change to occur at the interface instead of throughout the system.

### 3.4.2 Umbrella sampling constant

Finally, the size of the potential well can be changed through the use of a constant in equation 19,  $\kappa$ . The multiplicative increase or decrease of the potential well is another determining factor in deciding whether or not a system will experience local ordering in a bulk phase in which this is not expected, or experience an undesirable phase change in a bulk phase. For our simulations a number of umbrella sampling constants were used and their effects will later be discussed, their values are given below:

- $\kappa = 2$
- $\kappa = 1$
- $\kappa = 0.5$
- $\kappa = 0.2$

With this all the computational methods necessary for the simulation have been discussed so the simulation can proceed if the right parameters are provided, as will be discussed below.

## 3.5 Parameters

The only parameters necessary to reproduce the Monte Carlo simulation with the same techniques, that is an constant NPT configuration, a Weeks-Chandler-Andersen interaction potential, and performed in an elongated box to ensure bulk phases are present, are the number of particles, temperature, pressure. These are given as:

- Number of Particles,  $N = 977$
- Temperature,  $k_B T = 0.025\epsilon$
- Pressure,  $P = 0.22175\epsilon\sigma^{-3}$

where  $\epsilon$  is the unit of energy and  $\sigma$  is the unit of length. The temperature and pressure are chosen such that the system is in equilibrium for both the FCC-crystalline phase as well as the fluid phase.

Subsequently an umbrella sampling constant  $\kappa$  was chosen. Finally the umbrella sampling target bond order parameters are the last piece of information, as seen in equation 19. For our simulations, a number of different target bond order parameters were chosen. For all these cases the umbrella sampling constant  $\kappa$  was varied.

One case where the target bond order parameters are defined as follows:

$$\bar{q}_{l,target} = \frac{1}{2} * \bar{q}_{l,FCC} + \frac{1}{2} * \bar{q}_{l,fluid} \quad (20)$$

wherewith FCC is meant to refer to the values of the averaged bond order parameters of the FCC phase as denoted in table 1, and *fluid* is meant to refer to the values of the averaged bond order parameters of the liquid phase as denoted in that same table, and  $\bar{q}_{target}$  refers to  $\bar{q}_{l,target}$  for unspecified  $l$  which makes it applicable to both cases of  $l = 4$  or  $l = 6$ .

For the target bond order parameter of  $l = 6$ , this becomes  $\bar{q}_{6,target} = \frac{1}{2} * \bar{q}_{6,FCC} + \frac{1}{2} * \bar{q}_{6,fluid} = 0.094713$

A second case where the target bond order parameters are defined as:

$$\bar{q}_{target} = \frac{3}{4} * \bar{q}_{l,FCC} + \frac{1}{4} * \bar{q}_{l,fluid} \quad (21)$$

with the same parameters as above. Here, for the target bond order parameter of  $l = 6$ , this becomes  $\bar{q}_{6,target} = \frac{3}{4} * \bar{q}_{6,FCC} + \frac{1}{4} * \bar{q}_{6,fluid} = 0.409029$ .

And finally a third case where the target bond order parameters are defined as:

$$\bar{q}_{target} = \frac{1}{4} * \bar{q}_{l,FCC} + \frac{3}{4} * \bar{q}_{l,fluid} \quad (22)$$

with the same parameters as equation 20. for the target bond order parameter of  $l = 6$ , this becomes  $\bar{q}_{6,target} = \frac{1}{4} * \bar{q}_{6,FCC} + \frac{3}{4} * \bar{q}_{6,fluid} = 0.244318$ .

The umbrella sampling constant  $\kappa$  from equation 19 was also varied to determine the value for which the system is still impacted by umbrella sampling yet does not induce phase changes throughout or local ordering in a bulk phase of the system.

With this all the simulations have been defined and could be executed. The results were gathered and will be discussed below.

## 4 Results and Discussion

As mentioned above three cases were ran, all at the same temperature and pressure parameters, with the same number of particles, differing only in the usage of umbrella sampling target parameters:

- Umbrella sampling with target bond order parameters:  $\bar{q}_{l,target} = \frac{1}{2} * \bar{q}_{l,FCC} + \frac{1}{2} * \bar{q}_{l,fluid}$
- Umbrella sampling with target bond order parameters:  $\bar{q}_{l,target} = \frac{3}{4} * \bar{q}_{l,FCC} + \frac{1}{4} * \bar{q}_{l,fluid}$
- Umbrella sampling with target bond order parameters:  $\bar{q}_{l,target} = \frac{1}{4} * \bar{q}_{l,FCC} + \frac{3}{4} * \bar{q}_{l,fluid}$

Each case being ran for four different umbrella sampling constants  $\kappa$ , namely  $\kappa = 0.2, 0.5, 1, 2$ , which is used in equation 19. Due to the large number of results of the cases, the three cases will be discussed using only a single umbrella sampling constant  $\kappa$ . Subsequently the case of  $\bar{q}_{l,target} = \frac{1}{4} * \bar{q}_{l,FCC} + \frac{3}{4} * \bar{q}_{l,fluid}$  will be discussed for each umbrella sampling  $\kappa$  and consequently compared in the context of the interface and the effects of umbrella sampling on the interface. In order to reduce correlation effects one snapshot every twenty Monte Carlo volume moves, or Monte Carlo cycles, was taken. The simulations were generally ran for 7000 to 10000 Monte Carlo cycles to ensure the system could equilibrate, resulting in 350 to 500 snapshots for each simulation.

Described below are the three cases, which will first be analysed by looking at the bond order parameters for  $l = 4$  and  $l = 6$  and if they are able to distinguish the present phases properly. Next will be looked at umbrella sampling and its impact on the system, focussing on whether or not the system has been moved properly by umbrella sampling. Finally looking at the case of  $\bar{q}_{l,target} = \frac{1}{4} * \bar{q}_{l,FCC} + \frac{3}{4} * \bar{q}_{l,fluid}$  where all the umbrella sampling constants are compared, we might be able to determine the effects of the umbrella sampling constant on umbrella sampling. This will aid us in concluding whether or not umbrella sampling is able to shift the location of the interface properly.

### 4.1 Case: $\frac{1}{2} \bar{q}_{l,FCC} + \frac{1}{2} \bar{q}_{l,fluid}$ ; $\kappa = 0.2$

The two-phase fluid-solid system with the umbrella sampling target bond order parameters set to  $\bar{q}_{target} = \frac{1}{2} \bar{q}_{6,FCC} + \frac{1}{2} \bar{q}_{6,fluid} = 0.3116735$ , recognizing that under the given equilibrium conditions the system should not melt or crystallize further and that the interface is free to move without umbrella sampling, however with umbrella sampling it should remain at its given location and was expected to have no further change occurring throughout the system. For each umbrella sampling constant, the simulation remained stable, being that the interface did not stray from its original location and neither of the phases underwent a phase change or experienced any local ordering.

Discussed below is the simulation with the umbrella sampling constant  $\kappa = 0.2$

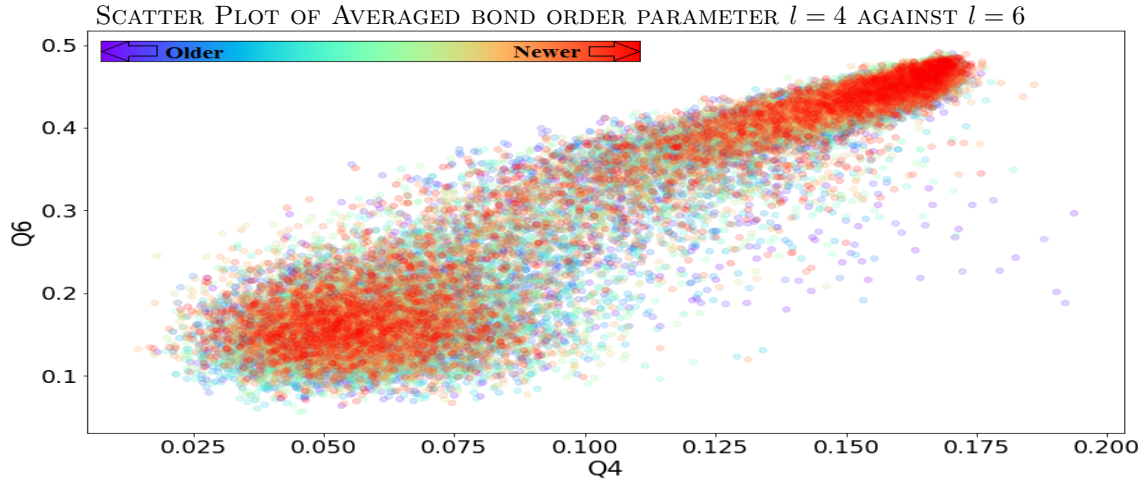


Figure 1:  $\bar{q}_4$  and  $\bar{q}_6$  data points from all snapshots. The bulk FCC phase is depicted on the right top side, the bulk fluid phase is depicted at the left bottom side..

Figure 1 shows that the two phases can clearly be distinguished from each other using the averaged local bond order parameters. The interface has wide ranging values starting off from the upper end of the tail of the FCC phase moving down on the bulk fluid phase. This does not occur as a straight line but instead the data points approach the bulk fluid phase through a curve reaching the upper part of the bulk fluid phase. Thus the interface is not a straight line between the two phases but instead a curve retaining FCC characteristics longer than it does fluid characteristics. Since we can distinguish the different phases using bond order parameters we can continue to examine the change brought on by umbrella sampling.

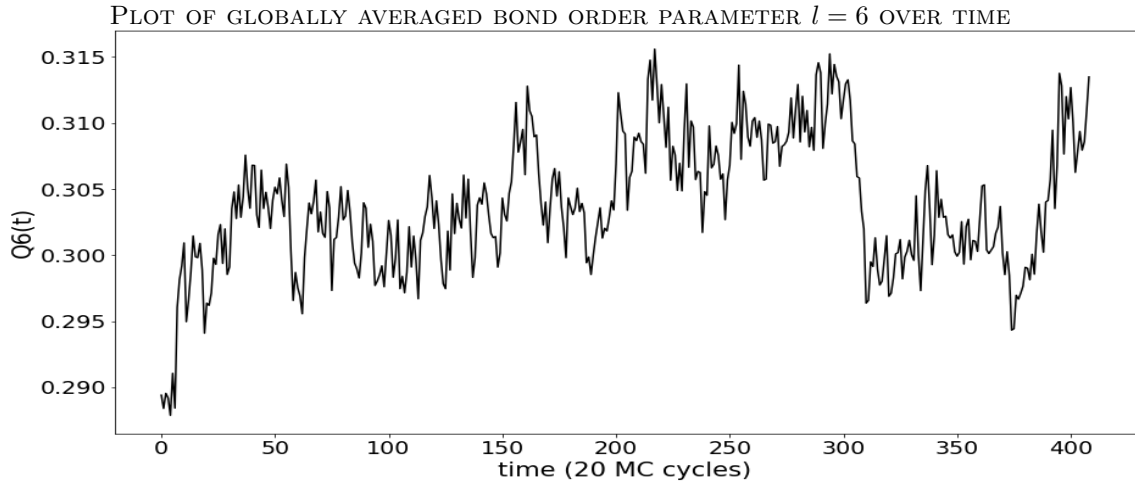


Figure 2: Globally averaged  $\bar{q}_6$  per snapshot. Only small variation occurs as expected since the interface is not supposed to shift location.

From figure 2 it can be seen that the system approaches its target value of 0.3116735. The system ran for a total of 8000 MC cycles, resulting in 400 files to be analyzed. Considering that the

variation of  $\bar{q}_6$  remains small over time, it is fair to assume that the system has equilibrated, despite the deviations over time of the global bond order parameter from the bond order parameter target value the system experiences as seen in the figure.

Data for umbrella sampling constants  $\kappa = 0.5, 1, 2$  all have the same characteristics and have remained stable, continuing to keep the interface at the same location. For larger values the bond order parameter target values are reached faster, and to some degree less deviation of the global bond order parameter from the bond order parameter target is observed. From figure 2, it appears that the umbrella sampling works well to keep the interface at its specific location, and from figure 1 it also seems the bulk phases are retained. From the following figures can be analysed whether or not the system retains both phases in the ratio that is expected, or that changes occur in the bulk through local (dis)ordering due to umbrella sampling.

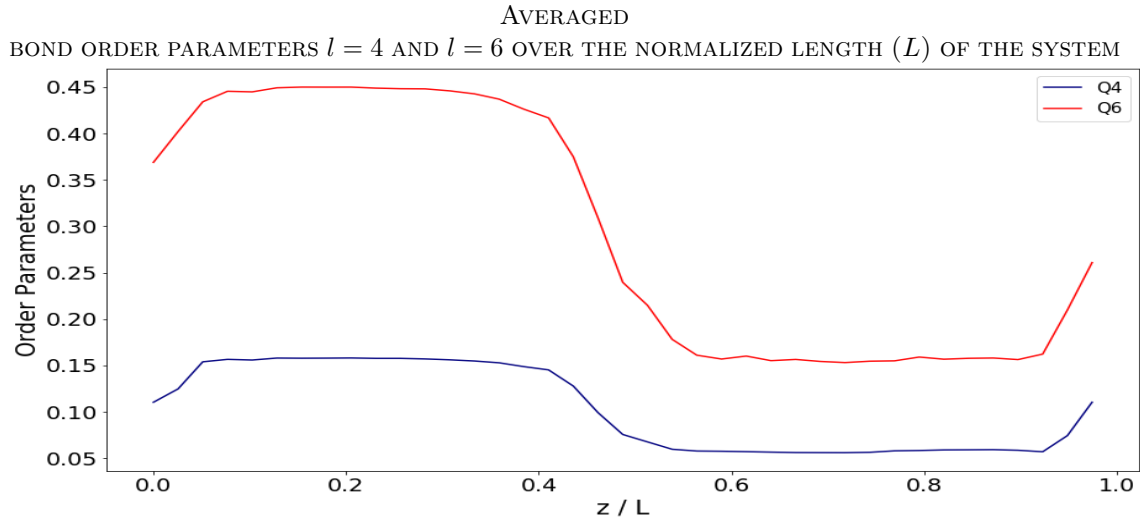


Figure 3:  $\bar{q}_4$  and  $\bar{q}_6$  averaged over all the snapshots after equilibrium has been attained.

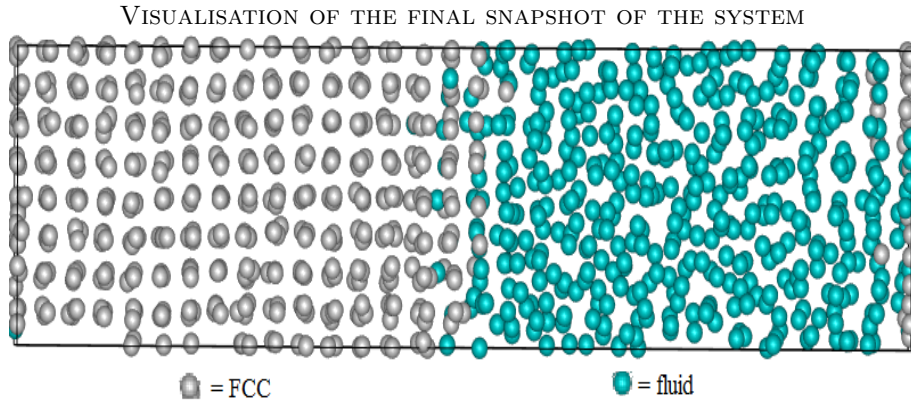


Figure 4: Colouring is determined by  $\bar{q}_6 > 0.3$  to achieve a rough indication of what constitutes the FCC-phase

Using figures 3 and 4 it becomes clear that the expected ratio is retained. There are two clear bulk phases, on the left the FCC phase which is well ordered in a crystal structure, and on the right the disordered fluid phase. No local ordering is observed in the FCC phase indicating that at this umbrella sampling constant no bulk phase transitioning is occurring. At the edges of the  $z$ -axis, where there are no periodic boundary conditions but hard wall conditions (unlike the  $x$ - and  $y$ -axes), the number of connections drop off for both the FCC and fluid phase. This causes a drop in bond order parameters in the beginning of the FCC-phase which is caused by local disordering since the FCC-particles at that edge can no longer be considered a bulk phase. In the same way the bond order parameters at the end of the fluid-phase are raised and local ordering starts to form. It is unknown why exactly the local ordering occurs, but the particles located at that edge can no longer be considered to be part of a bulk fluid phase, so this irregular behaviour was expected.

SCATTER PLOT OF AVERAGED BOND ORDER PARAMETER  $l = 6$  OVER THE NORMALIZED LENGTH ( $L$ ) OF THE SYSTEM

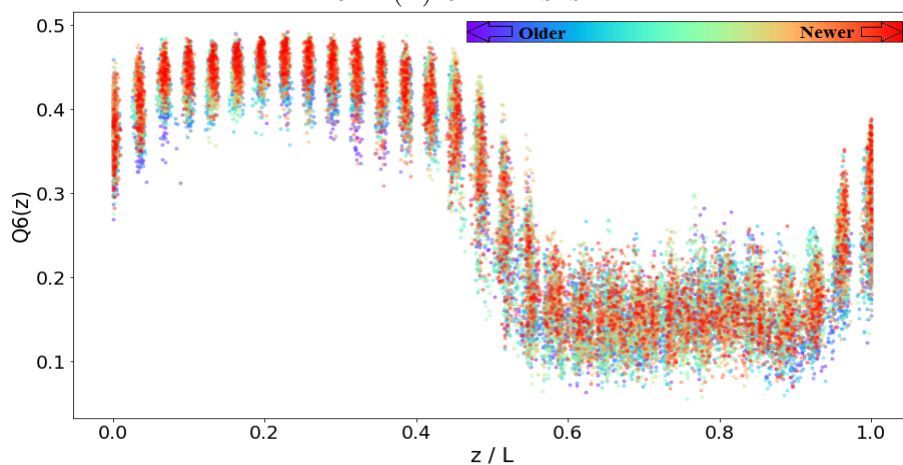


Figure 5:  $\bar{q}_6$  data points from the last 30 snapshots over the normalized length of the box.

Finally from figure 5, we can see how the system has behaved during the last 30 snapshots. It tells us whether or not any changes occurred in the time during which we expected to see an equilibrated system. The bulk phases do not seem to differ much over time, as both the FCC phase remains steady at its current bond order parameter values, as well as the fluid phase which seems to retain its disordered state over during the snapshots from which this figure was made. The figure shows that the system did attain equilibrium and retained it over time, as was implied from figure 2.

Clearly umbrella sampling has been able to retain the location of the interface, pushing the system towards the target values while ensuring the bulk phases experience no bulk phase transitions. However this is just for the case of  $\frac{1}{2} \bar{q}_{l,FCC} + \frac{1}{2} \bar{q}_{l,fluid}$ , and the expectation of umbrella sampling is that it is able to shift the location of the interface without causing bulk phase transitions. This case serves as a way of comparing the next two cases, in which the target parameters are changed to cause a shift in the location of the interface, to ascertain whether or not the shifting is done successfully or not.



## 4.2 Case: $\frac{3}{4}\bar{q}_{l,FCC} + \frac{1}{4}\bar{q}_{l,fluid}$ ; $\kappa = 0.2$

For the case of  $\bar{q}_{target} = \frac{3}{4}\bar{q}_{6,FCC} + \frac{1}{4}\bar{q}_{6,fluid} = 0.40903$ , the system starts off with half of the system in the FCC phase and the other half in the fluid phase. We expect the location of the interface to shift during the simulation, crystallizing a part of the fluid phase while the interface moves into the fluid phase due to the influence of umbrella sampling. We discuss the simulation with the umbrella sampling constant  $\kappa = 0.2$ .

Higher values of the umbrella sampling constant,  $\kappa = 0.5, 1, 2$  have induced local ordering in the fluid phase. The umbrella sampling potential for higher umbrella sampling constants had too much of an impact and induced effects in the bulk phases, especially the bulk fluid phase. This stretched out the interface as the bond order parameter target values were achieved by this local ordering instead of the proper shifting of the location of the interface. For the lower umbrella sampling constant of  $\kappa = 0.2$ , the system was steadily, albeit very slowly growing towards its target values, but did not reach those after 7000 MC cycles. The location of the interface was shifted and the interface was not stretched out, however it had not yet achieved a configuration where 75% of the system consisted of the FCC phase.

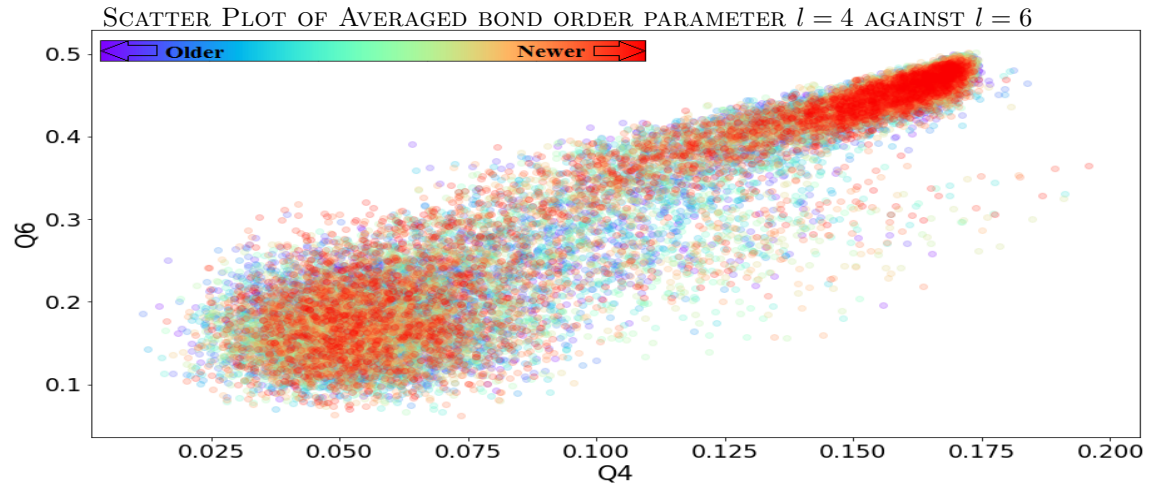


Figure 6:  $\bar{q}_4$  and  $\bar{q}_6$  data points from all snapshots. The bulk FCC phase is depicted on the right top side, the bulk fluid phase is depicted at the left bottom side..

Figure 6 shows that the two phases remain separate. The bulk fluid phase has not made an upwards transition but has narrowed in its range of  $\bar{q}_4$  by a small margin. The interface has the same curve as for the case of  $\bar{q}_{target} = \frac{1}{2}\bar{q}_{l,FCC} + \frac{1}{2}\bar{q}_{l,fluid}$  as was seen in figure 1. Higher values of the umbrella sampling constant showed an upward movement of the bulk fluid phase due to the large impact of the umbrella sampling potential.

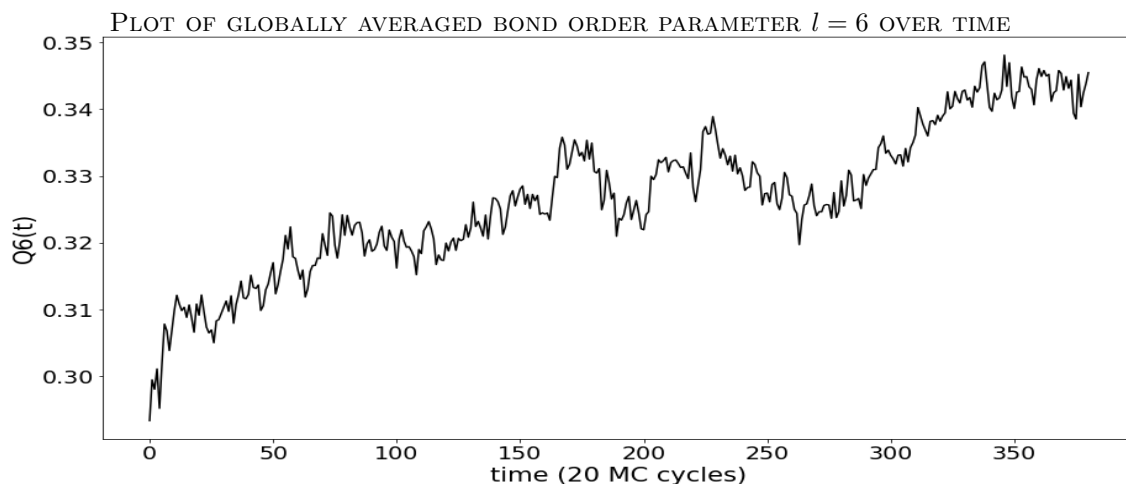


Figure 7: Globally averaged  $\bar{q}_6$  per snapshot. The bond order parameter target values were not achieved after 7000 MC cycles, instead the system kept steadily increasing.

From figure 7 it can be seen that the system is growing its target value of 0.40903. The system ran for a total of 7000 MC cycles, resulting in 350 files to be analyzed. The averaged bond order parameter of  $\bar{q}_6$  kept steadily increasing during that time, however its increase was very slow. This was not unexpected, crystal growth simulation appears to occur on longer timescales than crystal melting, possibly due to the high level of ordering that needs to be achieved requiring all the particles to be moved into exactly the right positions, whereas the disordered fluid phase on the other hand is easier achieved.

For larger values of the umbrella sampling constant, bond order parameter target values were approached faster, but invariably induced local ordering in the fluid phase. The induced umbrella sampling potential was too large to merely shift the interface, but instead stretched it out while locally ordering the fluid phase to achieve the bond order parameter target values as quickly as possible to decrease the potential the system was under. From the following figures it can be seen whether or not any local ordering occurred in the system.

AVERAGED  
BOND ORDER PARAMETERS  $l = 4$  AND  $l = 6$  OVER THE NORMALIZED LENGTH ( $L$ ) OF THE SYSTEM

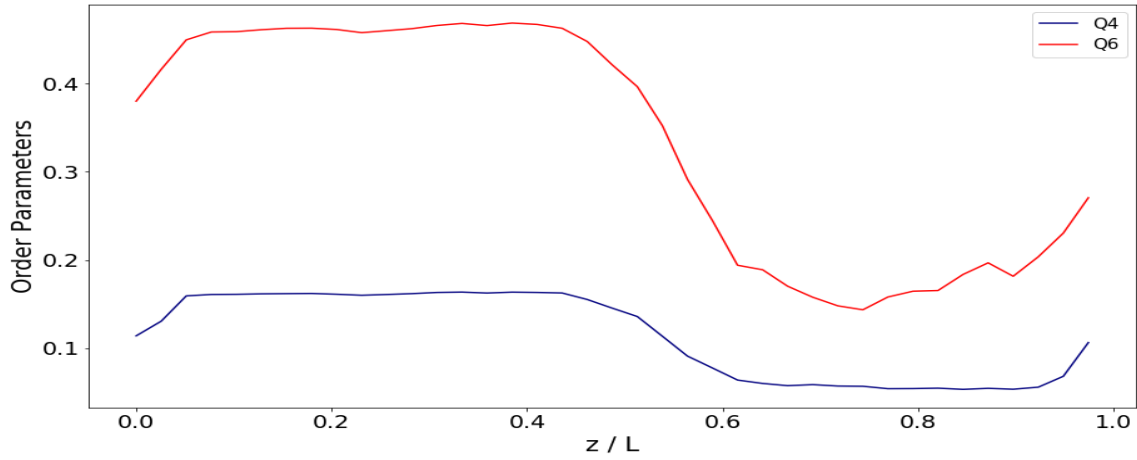


Figure 8:  $\bar{q}_4$  and  $\bar{q}_6$  averaged over all the snapshots after equilibrium has been attained.

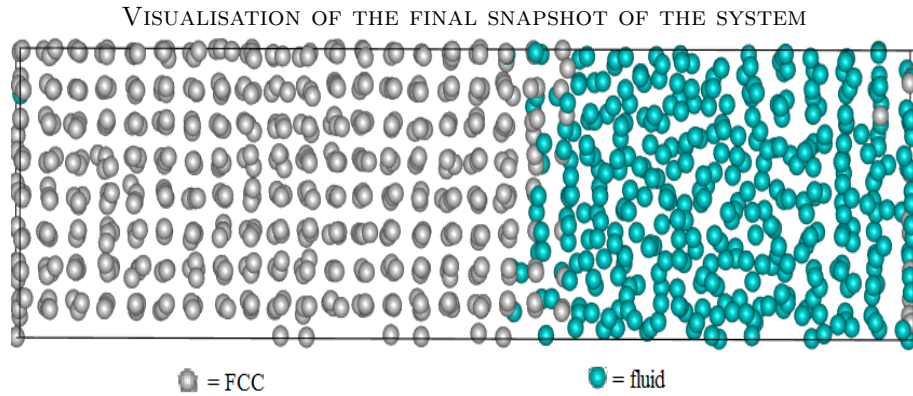


Figure 9: Colouring is determined by  $\bar{q}_6 > 0.3$  to achieve a rough indication of what constitutes the FCC-phase

Using figures 8 and 9 and comparing it to figures 3 and 4, there is clear growth towards the target ratio of 75% FCC. However this is not achieved as could already be deduced from figure 7. No local ordering is observed in the fluid phase indicating that at this umbrella sampling constant no bulk phase transitioning is occurring. At the edges of the  $z$ -axis, where there are no periodic boundary conditions but hard wall conditions (unlike the  $x$ - and  $y$ -axes), we again observe the effects of a decreased number of connections.

Despite not achieving the target ratio, the system does not suffer from local ordering and is clearly still growing towards the target values. On a longer timescale, the system is thus expected to achieve the bond order parameter target values.

Finally the scatter plot of the averaged bond order parameters over the length of the system might indicate if there has been any local ordering within the fluid phase. If the fluid phase does

not look disordered in its bulk phase, we might conclude local ordering has occurred which would lead to a stretched out interface and not a final system consisting of 75% FCC phase.

SCATTER PLOT OF AVERAGED BOND ORDER PARAMETER  $l = 6$  OVER THE NORMALIZED LENGTH ( $L$ ) OF THE SYSTEM

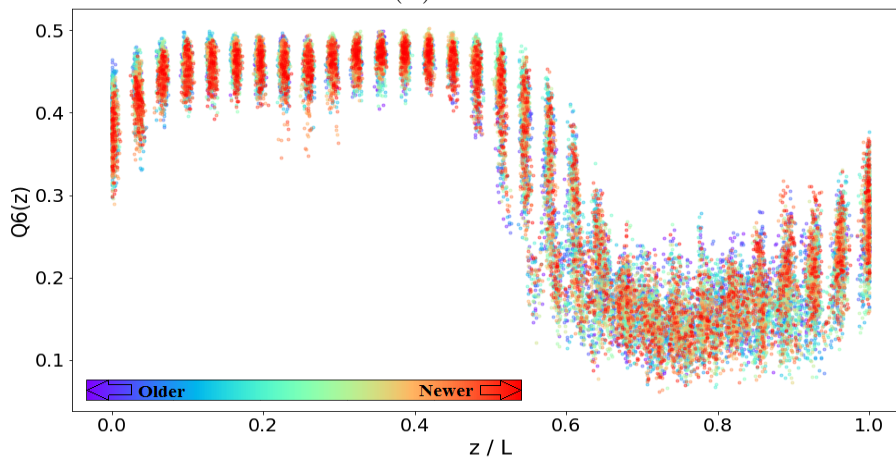


Figure 10:  $\bar{q}_6$  data points from the last 30 snapshots over the normalized length of the box.

Finally from figure 10, made over the last 30 snapshots, we see that there has been no local ordering occurring in the bulk fluid phase. Instead both bulk phases retain their characteristics over time, while the interface keeps slowly moving to the right as particles of the fluid phase close to the interface crystallize into the FCC phase.

Umbrella sampling has clearly been able to shift the location of the interface, pushing the system towards the target values while ensuring the bulk phases experience no bulk phase transitions in the form of local ordering. However, this is for the case of the umbrella sampling constant of  $\kappa = 0.2$ , causing the system to only gradually grow towards the bond order parameter target values. For higher values the local ordering observed was an obstruction for the proper shifting of the interface, so that if umbrella sampling is to be applied, a small umbrella sampling constant becomes necessary to ensure both bulk phases are kept.

### 4.3 Case: $\frac{1}{4} \bar{q}_{l,FCC} + \frac{3}{4} \bar{q}_{l,fluid}$ ; $\kappa = 0.5$

For the case of  $\bar{q}_{target} = \frac{1}{4} \bar{q}_{6,FCC} + \frac{3}{4} \bar{q}_{6,fluid} = 0.244318$ , the system starts off with half of the system in the FCC phase and the other half in the fluid phase, in the same way as the previous two cases. The location of the interface shifted during the simulation, as expected, melting a part of the FCC phase as the interface moved into the FCC phase due to umbrella sampling. We discuss the simulation with the umbrella sampling constant  $\kappa = 0.5$ .

The lower value of the umbrella sampling constant,  $\kappa = 0.2$  took a very long time to melt the FCC phase, while the process did not induce local disordering for the umbrella sampling constant  $\kappa = 0.5$ , so that one was chosen for discussion. Higher values of the umbrella sampling constant,  $\kappa = 1, 2$  have induced local disordering in the FCC phase. The umbrella sampling potential for higher umbrella sampling constants had too much of an impact, exacerbating the local disordering at the wall of the system at the FCC phase, decreasing the bond order parameter values. On

the side of the interface, the FCC phase was affected by the large umbrella sampling potential, stretching out the interface as the system tried to achieve the bond order parameter target values. The system ran for 9000 MC cycles, achieving a value very close to equilibrium after a 1000 MC cycles. The location of the interface was shifted, and not stretched out, achieving a configuration where 25% of the system remained FCC while 75% of the system ended up as a bulk fluid phase.

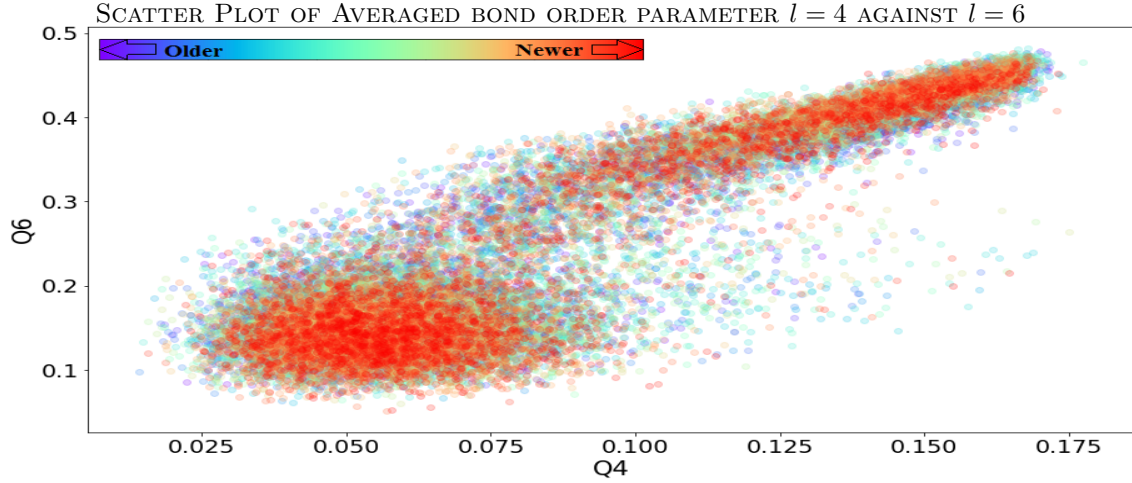


Figure 11:  $\bar{q}_4$  and  $\bar{q}_6$  data points from all snapshots. The bulk FCC phase is depicted on the right top side, the bulk fluid phase is depicted at the left bottom side..

Figure 11 shows us that both phases remained present as separate bulk phases. No bulk phase transitions are observable. Higher values of the umbrella sampling constant depict a downwards transition of the bulk FCC phase towards the bulk fluid phase indicating local disordering due to the large impact of the umbrella sampling potential. With both phases retained, we can continue to the development of the bond order parameter over time.

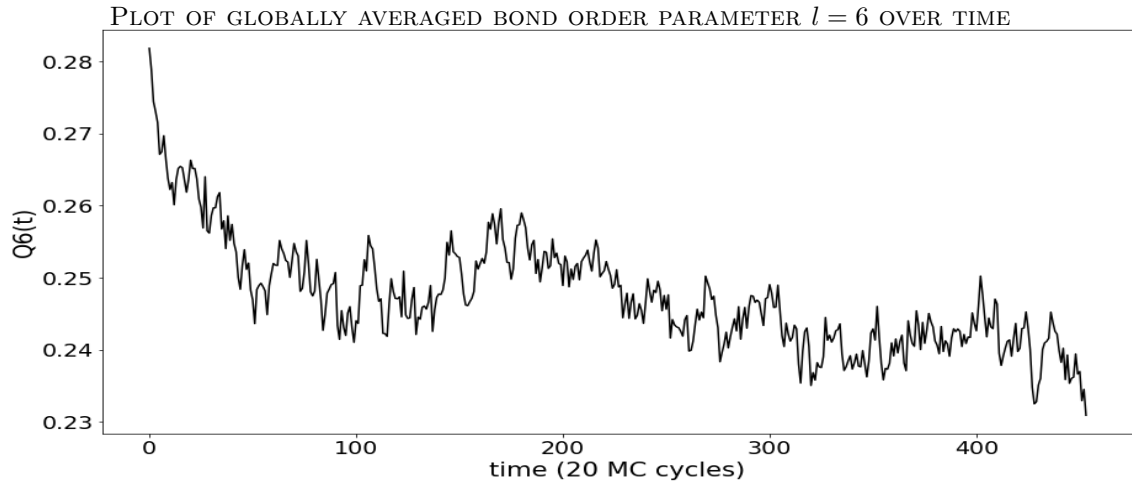


Figure 12: Globally averaged  $\bar{q}_6$  per snapshot. The bond order parameter target values were achieved after roughly a 1000 MC cycles.

Figure 12 shows the globally averaged bond order parameter of  $\bar{q}_6$  reaching the bond order parameter target value of 0.244318. The system ran for a total of 9000 MC cycles, attaining equilibrium after roughly 500 MC cycles. It seems that crystal melting simulations occur on a shorter timescale than do crystal growth simulations.

Larger values of the umbrella sampling constant resulted in an even shorter timescale in which the bond order parameter target values were achieved, however this tended to induce local disordering effects in the bulk FCC phase. From the following figures pertaining to the visualisation we can see if local disordering occurred in the bulk FCC phase.

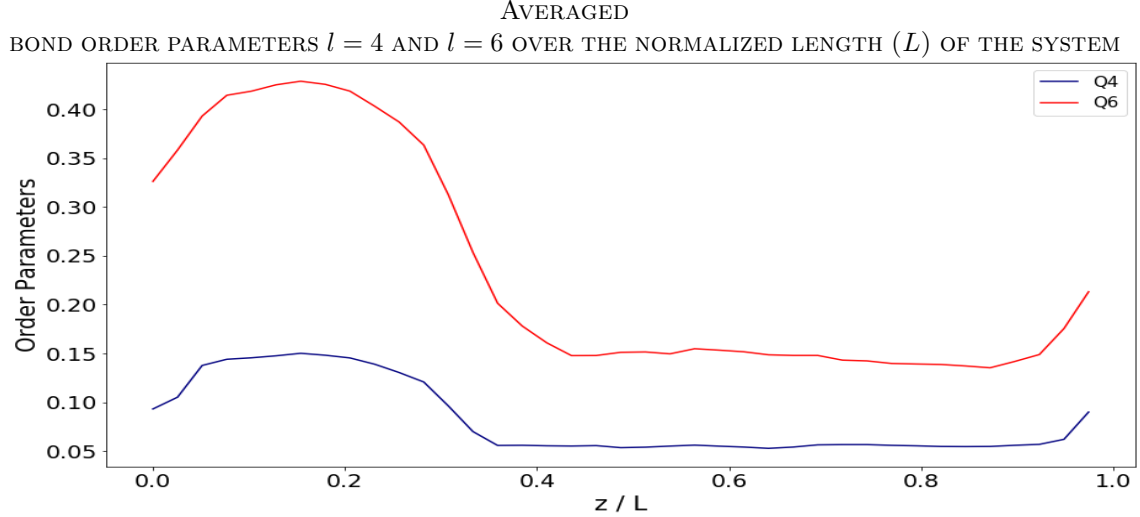


Figure 13:  $\bar{q}_4$  and  $\bar{q}_6$  averaged over all the snapshots after equilibrium has been attained.

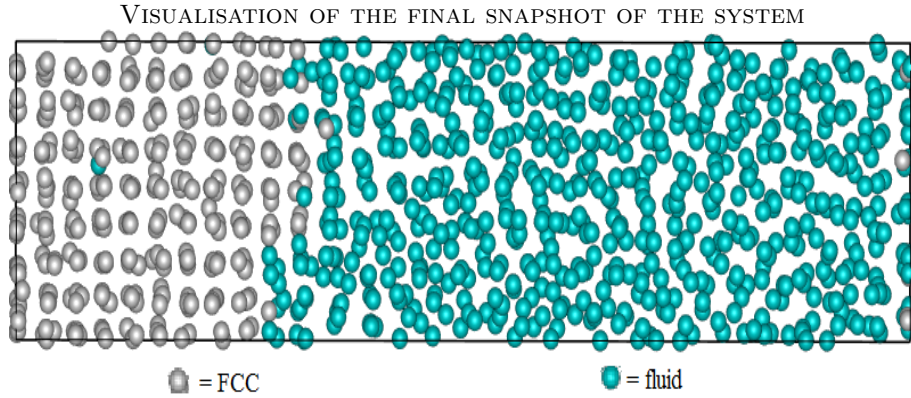


Figure 14: Colouring is determined by  $\bar{q}_6 > 0.3$  to achieve a rough indication of what constitutes the FCC-phase

Comparing figures 13 and 14 to figures 3 and 4, there is clear crystal melting occurring, achieving the target ratio of 25% FCC. No local disordering occurs in the bulk FCC phase, except for the known disordering on the edge of the FCC phase at the wall due to the hard wall conditions. The

system remains stable, and from figure 14 we can clearly see that 25% of the system is retained as FCC whilst the rest has become a fluid phase.

The following scatter plot of the averaged bond order parameters over the length of the system will further indicate if the system has achieved an equilibrium, and serves as a final check as to whether there is local disordering in the FCC phase.

SCATTER PLOT OF AVERAGED BOND ORDER PARAMETER  $l = 6$  OVER THE NORMALIZED LENGTH ( $L$ ) OF THE SYSTEM

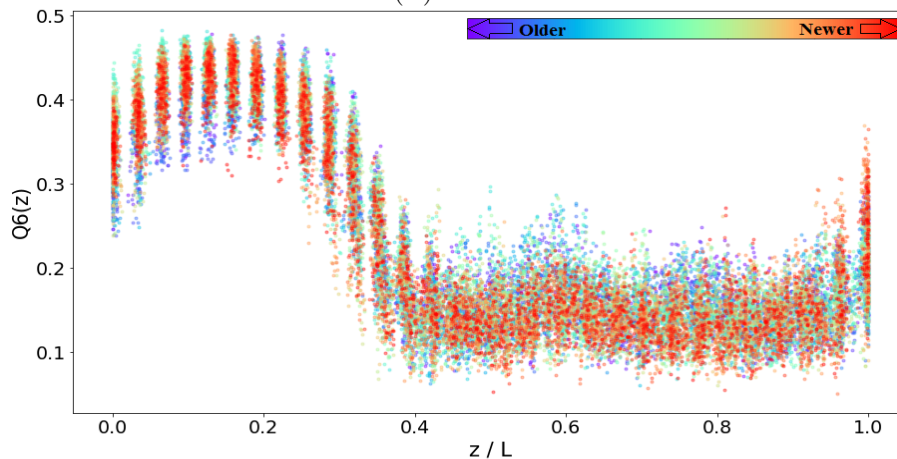


Figure 15:  $\bar{q}_6$  data points from the last 30 snapshots over the normalized length of the box.

Figure 15 of all the data points over the last 30 snapshots shows us that there is hardly any change in the system. It has equilibrated and is now a stable 25% FCC and 75% fluid system, as was expected. Both phases retain their characteristics, and only the FCC phase at the edge of the wall has some decreased values, despite that it retains FCC characteristics.

In this case as well, umbrella sampling shows itself capable of shifting the interface towards the desired bond order parameter target values, without inducing local disordering in the bulk FCC phase. The simulation with umbrella sampling constant  $\kappa = 0.2$  probably would achieve the same result, albeit over a longer timescale. For the simulations with higher umbrella sampling constants,  $\kappa = 1, 2$ , we see stretched out interfaces and local disordering decreasing the bond order parameter values for the FCC phase as the umbrella sampling potential forces the bulk phase to transition as the potential is too large. However as opposed to the case of  $\bar{q}_{target} = \frac{3}{4}\bar{q}_{l,FCC} + \frac{1}{4}\bar{q}_{l,fluid}$ , where a lower value of the umbrella sampling constant is desired, for the case of crystal melting, a higher umbrella sampling constant can be used. This results in target values being achieved on a shorter timescale, leading to a decreased computation time.

#### 4.4 Case: $\frac{1}{4}\bar{q}_{l,FCC} + \frac{3}{4}\bar{q}_{l,fluid}$ ; All umbrella sampling constants

Finally, to see how the umbrella sampling constant variation affects the simulations, the third case with the bond order parameter target value of  $\bar{q}_{target} = \frac{1}{4}\bar{q}_{6,FCC} + \frac{3}{4}\bar{q}_{6,fluid} = 0.244318$  will be further examined for all the given umbrella sampling constants,  $\kappa = 0.2, 0.5, 1, 2$ . The comparison will focus on the effects of the differing umbrella sampling constant on the interface and the bulk phases.

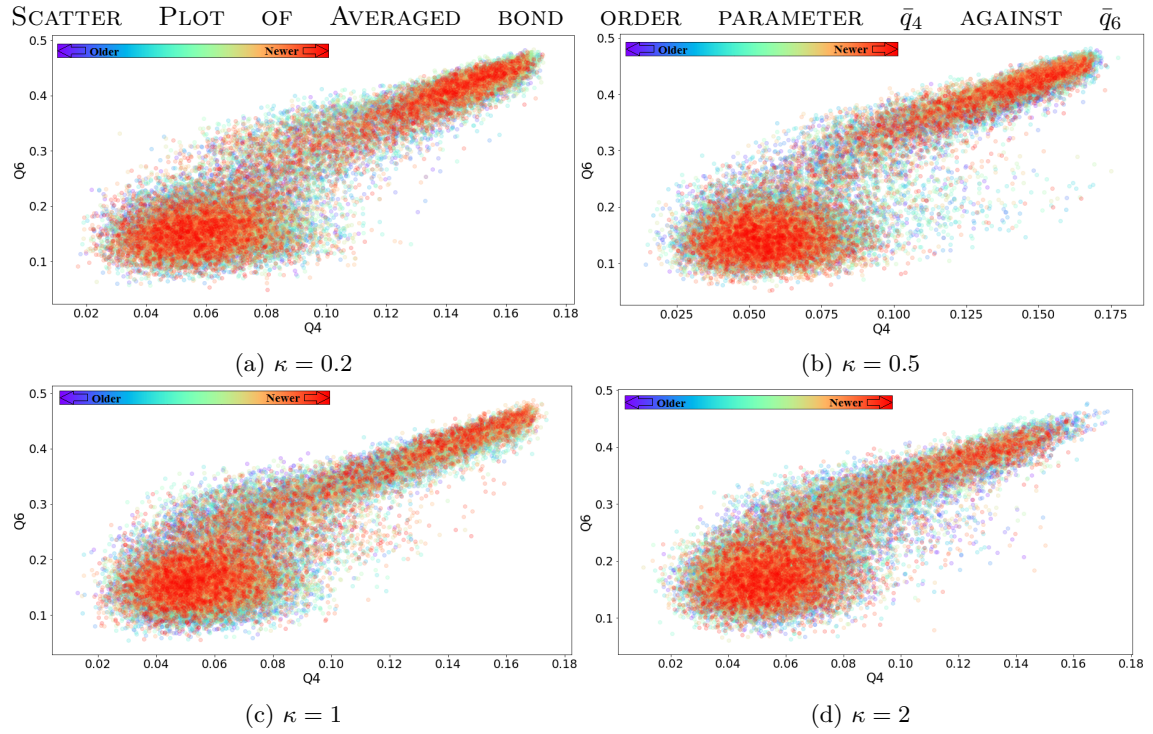


Figure 16:  $\bar{q}_4$  and  $\bar{q}_6$  averaged over all snapshots over the normalized length  $L$  of the box.

Figure 16 shows that for higher umbrella sampling constants some of the bulk FCC phase transitions downwards towards the bulk fluid phase, denoting the local disordering induced by larger umbrella sampling constants. However for  $\kappa = 0.2, 0.5$ , both phases are clearly retained.



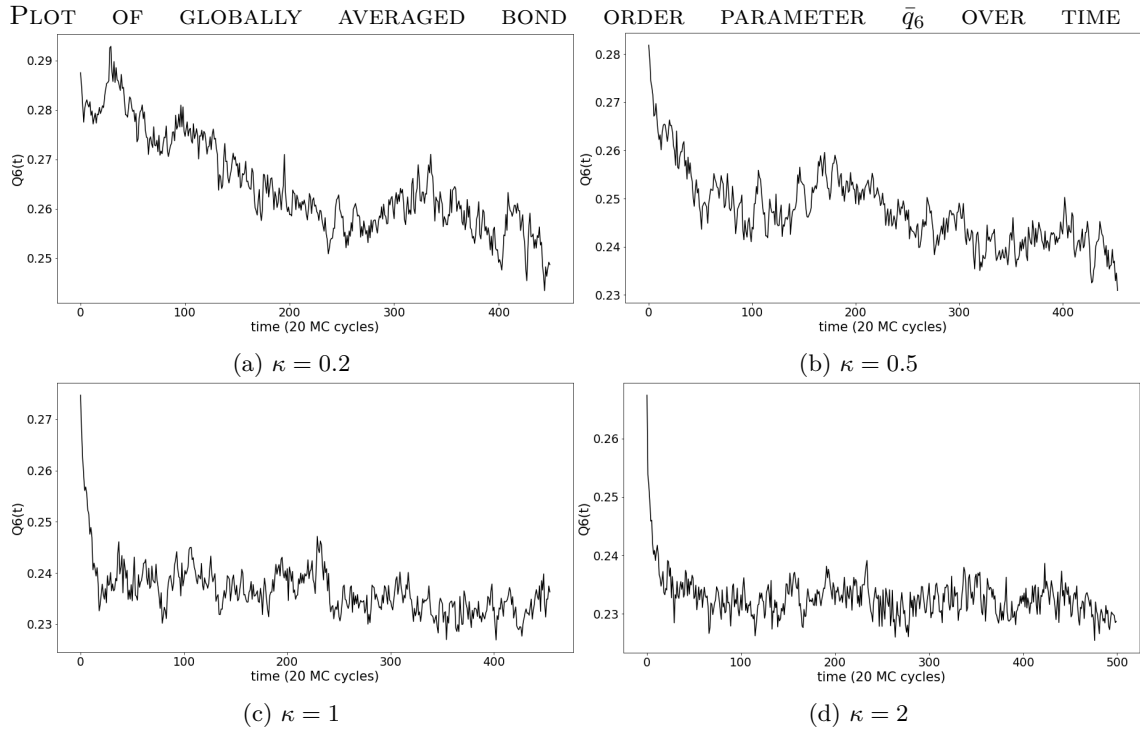


Figure 17: Globally averaged  $\bar{q}_6$  per snapshot.

Figure 17 depicts the global bond order parameter for  $l = 6$  over time for each umbrella sampling constant  $\kappa$ . Systems ran for 9000 MC cycles to 10000 MC cycles. Clearly for the cases with  $\kappa = 1, 2$ , seen in figures 17c and 17d, the bond order parameter target value is quickly reached and the system remains stable, even dipping below the target value. However for the lower values of the umbrella sampling constant, the global bond order parameter takes longer, for the case of  $\kappa = 0.2$ , it does not even reach the target value before the end of the simulation. However reaching the bond order parameter target values on a shorter timescale does not imply effective behaviour, as will be seen in later figures, due to the local disordering introduced by the larger umbrella sampling potential.

AVERAGED BOND ORDER PARAMETERS  $\bar{q}_4$  AND  $\bar{q}_6$  OVER THE NORMALIZED LENGTH( $L$ ) OF THE SYSTEM

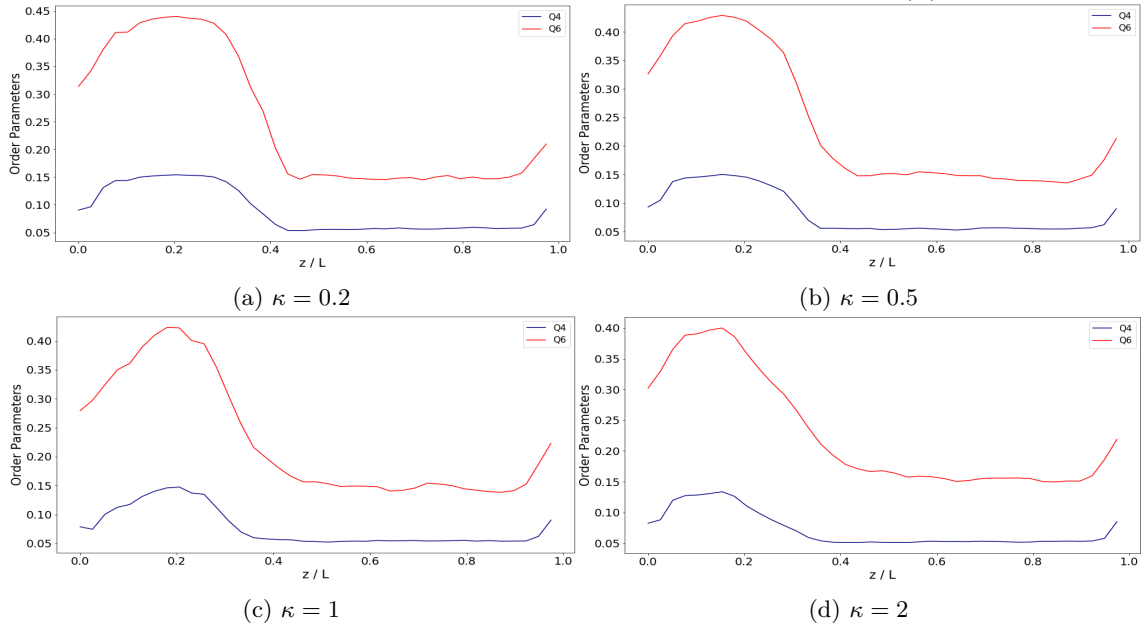


Figure 18:  $\bar{q}_4$  and  $\bar{q}_6$  averaged over all the snapshots after equilibrium has been attained.

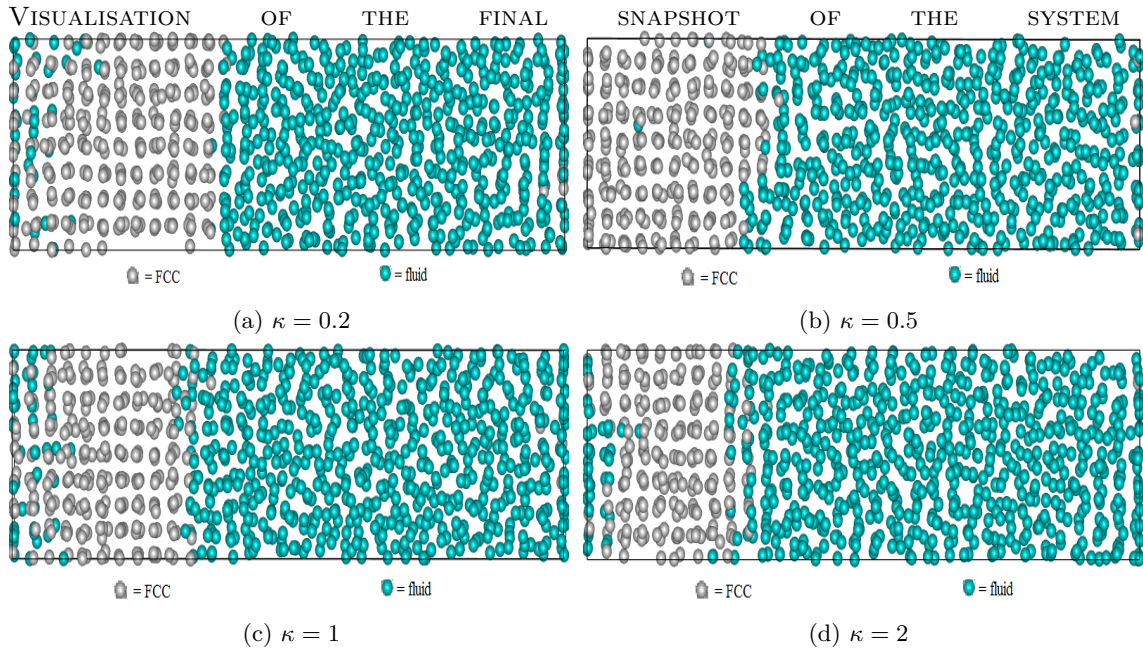


Figure 19: Colouring is determined by  $\bar{q}_6 > 0.3$  to achieve a rough indication of what constitutes the FCC-phase

When you compare the figures in figure 18 and figure 19, the effects of a large umbrella sampling

constant become even more clear. Local disordering induced by the larger umbrella sampling potential distort the already lowered bond order parameters at the edge of the FCC, at the hard wall. On top of that the interface becomes stretched out. This is seen in figures 19c and 19d, where at the interface both FCC particles and fluid particles have ended up mixing, whereas in figures 19a and 19b, and especially in figure 19a, the interface exhibits an almost strict distinction between the FCC phase and the fluid phase. The interface having become stretched out is problematic, as it has led to the global bond order parameter already achieving the target value by causing local disordering in the FCC phase while retaining some local ordering in the interface. This however has not occurred for the cases with lower umbrella sampling constant, that is  $\kappa = 0.2, 0.5$ . The interface in those simulations has not stretched out and the FCC phase has no local disordering. However both of these, looking at the figures of 19a and 19b, and at figures 17a and 17b, have not yet reached their target values. The FCC phase is still too large, covering almost a third instead of 25% of the system. The implication from figures 17a and 17b is that even more time is necessary to equilibrate the system, but from the other figures that the system will in fact equilibrate as an 25% FCC-75% fluid system if that time is provided.

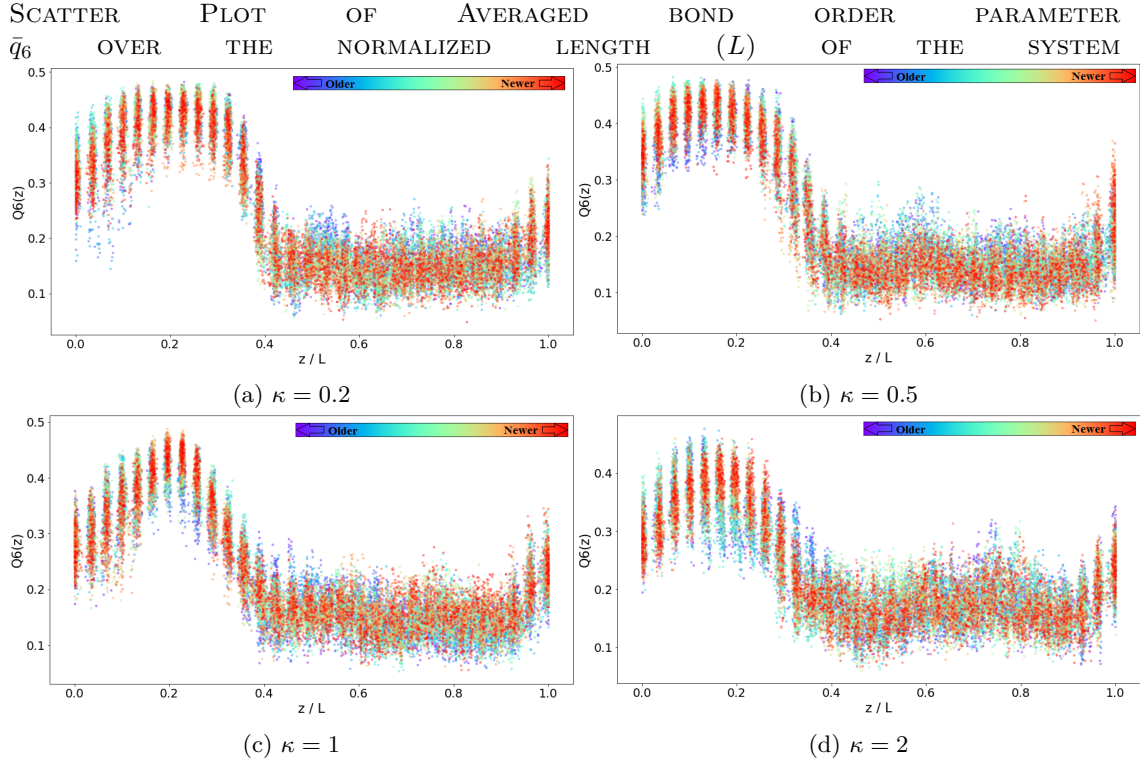


Figure 20:  $\bar{q}_6$  data points from the last 30 snapshots over the normalized length of the box.

Finally, using figure 20, the systems might appear roughly stable, however there appears to be some melting occurring as indicated by newer files depicting lower values in the interface for the cases of  $\kappa = 0.2, 0.5$ , however this effect is small, and 600 MC cycles does not appear to be a large enough measure to know for sure if that is occurring. The higher umbrella sampling constant cases of  $\kappa = 1, 2$  seem to show more disordering occurring at the edge of the FCC phase, at the wall. This might be the case as the  $\bar{q}_6$  over time figures of these cases, figures 17c and 17d

seem to have dipped below the target values. Perhaps the umbrella sampling potential is causing melting at the edge of the FCC phase at the wall, and due to the hard wall effects, is unable to reascertain the FCC phase there. To know for sure if the particles there will melt however, longer simulations will be necessary. Although for the past 9000 MC cycles after attaining the target values, there has been no actual melting of the FCC phase at the edge at the wall.

Having compared all the four umbrella sampling constants, a number of things become clear. A high umbrella sampling constant invariably induces such a large umbrella sampling potential that the interface becomes stretched, and that even for a low umbrella sampling potential (e.g.  $\kappa = 0.2$ ), the location of the interface is shifted, however the cost of using a low umbrella sampling potential is that it takes long timescale for the system to equilibrate. Using a too high umbrella sampling constant (e.g.  $\kappa = 1, 2$ ) however comes with the risk of inducing local ordering effects, which stretch out the interface, making subsequent analysis difficult.

## 5 Conclusion

Umbrella sampling has shown itself capable of shifting the location of the interface, as well as maintaining its current location without inducing effects in the bulk phases. Both crystal growth as well as crystal melting is possible with umbrella sampling. The most important factor in both crystal growth and in crystal melting has been the umbrella sampling constant  $\kappa$  from equation 19. Using a high umbrella sampling constant such as  $\kappa = 1, 2$ , local (dis)ordering is induced and the interface becomes stretched. However if a lower umbrella sampling constant is used, such as  $\kappa = 0.2, 0.5$ , this (dis)order does not occur, the interface does not become stretched, and both bulk phases retain their characteristics. This has as a drawback that it takes a much longer timescale for equilibrium to be reached.

As pertaining to the interface. Whenever a high umbrella sampling constant is used, the interface invariably ends up stretched out, making analysis difficult. With the use of a low umbrella sampling constant however, the interface remains sharp, only a few layers thick. This interface does not appear to go in a straight line as seen from the  $\bar{q}_4 - \bar{q}_6$ -figures, but appears to retain the FCC characteristics, reaching the bulk fluid phase downwards from the bulk FCC phase. However the interface does appear to go from one phase to the other, not having a defined set of bond order parameters associated with it.

As for the research questions asked in section 1.1:

1. How do the averaged local bond order parameters change with respect to an interface between a fluid and an FCC phase?

The interface between the FCC phase and the fluid phase seems to be a sharp transition between the two phases, only a few layers thick. If the umbrella sampling constant,  $\kappa$ , is larger than 1, and the target parameters are such that the interface requires to be shifted, the interface will end up stretched out due to the local (dis)ordering in the bulk phases. However at a small umbrella sampling constant,  $\kappa = 0.5, 0.2$ , the interface moves properly without stretching out. No local (dis)ordering is observed in those cases and the transition remains only a few layers thick. Finally the interface appears to retain more characteristics of the FCC phase in the form of a local ordering and higher bond order parameters for  $l = 6$ . However the interface does have characteristics of both bulk phases in which it is situated between.

2. Can umbrella sampling be used to shift the location of the interface?

Umbrella sampling has shown itself capable of shifting the location of the interface. However care needs to be taken that the introduced umbrella sampling potential is not large, mainly determined by the parameter of the umbrella sampling constant,  $\kappa$  as defined in equation 19. Generally if  $\kappa > 1$ , the umbrella sampling potential is too large and will induce local ordering during crystal growth and local disordering during crystal melting, causing a stretched out interface and deformed bulk phases, all of which are undesirable effects of umbrella sampling. However if the umbrella sampling constant is well chosen,  $\kappa \leq 0.5$ , no local ordering or local disordering will occur and both bulk phases will retain their characteristics. Especially the case of  $\kappa = 0.2$  seems to work for all cases. The advantage of choosing a lower umbrella sampling constant is the lower probability of introducing local (dis)ordering. The disadvantage of lowering the umbrella sampling constant is that this increases the computation time, so that achieving equilibrium occurs on a much longer timescale.

To fully grasp the consequences of umbrella sampling, the possibility of interface stretching and local (dis)ordering, and the impact of the umbrella sampling constant, more research is necessary. These simulations would have to be simulated for an umbrella sampling constant lower than 1 at least, and would have to be simulated on long timescales, probably exceeding 10000 Monte Carlo cycles in order for equilibrium to be achieved.

## Acknowledgements

I would like to express my appreciation for my daily supervisor, Gabriele Coli, for his patience and positive attitude regarding the thesis, for which I am grateful. I would also like to thank Professor Dijkstra for her continued support of the thesis. I found it a delightful learning experience. I wish to thank the department of Soft Condensed Matter and Inorganic Chemistry and Catalysis for the opportunity for the research project and I wish everyone success in their current or future projects.

## References

- [1] Stefan Auer and Daan Frenkel. Numerical simulation of crystal nucleation in colloids. In *Advanced Computer Simulation*, pages 149–208. Springer, 2005.
- [2] Marjolein Dijkstra. Modelling and simulation. Technical report, Soft Condensed Matter group, Debye Institute for Nanomaterials Science, University Utrecht, 2019.
- [3] W Keith Hastings. Monte carlo sampling methods using markov chains and their applications. 1970.
- [4] Wolfgang Lechner and Christoph Dellago. Accurate determination of crystal structures based on averaged local bond order parameters. *The Journal of chemical physics*, 129(11):114707, 2008.
- [5] Nicholas Metropolis, Arianna W Rosenbluth, Marshall N Rosenbluth, Augusta H Teller, and Edward Teller. Equation of state calculations by fast computing machines. *The journal of chemical physics*, 21(6):1087–1092, 1953.
- [6] Paul J Steinhardt, David R Nelson, and Marco Ronchetti. Bond-orientational order in liquids and glasses. *Physical Review B*, 28(2):784, 1983.
- [7] Glenn M Torrie and John P Valleau. Nonphysical sampling distributions in monte carlo free-energy estimation: Umbrella sampling. *Journal of Computational Physics*, 23(2):187–199, 1977.